Light Curve Analysis of Supernova AT2023hpb

Department of Physics, University of California, Santa Barbara, CA 93106

June 14, 2023

Abstract

This paper presents a brief analysis of the supernova light curve of AT2023hpb, aiming to gain insights into the behavior and characteristics of supernovae. By analyzing numerous photographs taken over a half-month period through the Las Cumbres Observatory Global Telescope Network (LCOGTN), the study examines the changes in supernova magnitude over time. It investigates the formation and types of supernovae, classification methods, observation techniques, and the significance of light curves in understanding these celestial events. The observed light curve of AT2023hpb reveals an initial decline in brightness followed by a subsequent increase, which is a characteristic feature of type II supernovae. The implications of these findings highlight the importance of light curve analysis in identifying and classifying supernovae and contribute to our understanding of these fascinating astronomical phenomena.

1 Introduction

Supernovae result from two primary mechanisms: the collapse of massive stars (Type II supernovae) and the thermonuclear explosion of white dwarfs (Type Ia supernovae) [1]. Type II supernovae occur when the iron core of a massive star collapses under its own gravity, leading to a powerful explosion [2]. Type Ia supernovae occur in binary star systems where a white dwarf accretes matter from a companion star. When the mass of the white dwarf reaches the Chandrasekhar limit, a runaway nuclear fusion process ignites, resulting in a catastrophic explosion [3].

Supernovae are classified based on their spectral features and light curve characteristics. Type II supernovae exhibit hydrogen lines in their spectra, indicating the presence of hydrogen-rich outer envelopes in their progenitor stars [4]. Type Ia supernovae, on the other hand, lack hydrogen lines and display strong silicon lines, indicating the explosion of a carbon-oxygen white dwarf [5]. Spectroscopic observations play a crucial role in determining the type and classifying supernovae by analyzing the absorption and emission lines present in their spectra.

Precise specification and observation of supernovae are essential for understanding their nature. Various telescopes and instruments, such as the Hubble Space Telescope and ground-based observatories, are employed for spectroscopic and photometric observations [6]. Spectroscopic observations provide valuable information about the chemical composition and velocity of the expanding material, allowing astronomers to study the elements synthesized in the supernova explosion [7]. Photometric observations involve measuring the supernova's brightness at different wavelengths over time, providing data points to construct the light curve [8].

The analysis of supernova light curves holds significant importance in various fields. Light curves provide crucial information about the physics of supernovae, aiding in the refinement of models and the understanding of the stellar explosion mechanism [9]. They offer insights into the energy released during the explosion, the composition of the ejected material, and the overall evolution of the supernova. Furthermore, light curves play a vital role in cosmological studies, allowing for the estimation of distances and the determination of cosmological parameters. The use of light curves in supernova surveys, such as the Supernova Legacy Survey, has contributed to the identification, classification, and study of large numbers of supernovae, providing valuable data for cosmological analyses [10].

The study of supernova light curves has also yielded insights into the nature of dark energy. Type Ia supernovae, with their well-characterized light curves, have been instrumental in measuring the accelerating expansion of the universe [11]. By analyzing the shape and magnitude of the light curves, researchers have derived cosmological parameters such as the matter density, dark energy density, and equation of state [12].

Additionally, the analysis of light curves allows for the determination of the intrinsic properties of supernovae, such as their luminosity and color. This information is crucial for calibrating distance indicators and refining our understanding of stellar evolution and nucleosynthesis processes [13]. By comparing the observed light curves with theoretical models, astronomers can study the progenitor stars, explosion mechanisms, and the impact of various factors on the observed properties of supernovae [14].

In summary, the analysis of supernova light curves through precise observation, classification, and mathematical modeling provides valuable insights into the formation, types, and evolution of these celestial events. Light curves serve as powerful tools for studying the physics, composition, and energy release during supernova explosions. Furthermore, they contribute to cosmological research by elucidating the expansion of the universe, aiding in the determination of cosmological parameters and the understanding of dark energy. The study of supernova light curves continues to deepen our understanding of the complex processes that shape our universe.

2 Method

This observational experiment began with an exploration of Purdue University's supernova database [15], which served as a valuable resource for identifying and studying various supernovae. Originally, the experiment was intended to observe two other supernovae, AT2023fnr and 2023dzc. However, due to some observation and processing issues with Las Cumbres Observatory (LCO), the data was compromised, and the peak brightness readings could not be retrieved. As a result, the decision was made to shift the observation project to a more recent supernova, AT2023hpb.

Some basic information about the supernova AT2023hpb is as follows: it was discovered on May 1, 2023, with a discovery magnitude of 14.2 [16]. AT2023hpb belongs to the CV type of supernova. Further details about AT2023hpb can be found on the Transient Name Server (TNS) [17].

We requested LCO to process the observation at its Observatory Sites LSC (Cerro Tololo Interamerican Observatory) and COJ (Siding Spring Observatory). The observation used 0.4-meter telescopes of LCO to observe AT2023hpb, starting from May 13, 2023. The filters SDSS g', SDSS r', and SDSS i' were employed, with an integration time of 100 seconds. The observation request sheet is shown in table 1.

Table 1: Observation Request for AT2023hpb

Target Name	RA (J2000)	Dec (J2000)	Filter	Exposures	Integration Times (s)	Observational Windows
AT2023hpb	00:51:11.790	-73:11:30.30	SDSS g'	2	100	Every 2 days (repeat for 2 weeks)
AT2023hpb	00:51:11.790	-73:11:30.30	SDSS i'	2	100	Every 2 days (repeat for 2 weeks)
AT2023hpb	00:51:11.790	-73:11:30.30	SDSS r'	2	100	Every 2 days (repeat for 2 weeks)

The raw images were processed using Astroart 8, which facilitated the geometry and astrometry process. Additionally, the software Atlas was employed to locate reference stars and accurately position AT2023hpb within the images.

To ensure consistency, images captured within the same observation period were selected for analysis. The star pattern method was utilized for auto alignment as part of the preprocessing stage. After noise reduction, the four brightest stars surrounding AT2023hpb were selected as reference stars in Atlas, with the coordinates obtained from GAIA DR2 (Figure 1). The selected reference stars underwent geometry and astrometry processing, yielding the reference star data presented in Table 2. Subsequently, the coordinates of AT2023hpb were determined based on the processed reference star frame, and Astroart 8 was employed for data processing. The processed data for AT2023hpb on May 11th and May 15th are depicted in Figure 2 and Figure 3, respectively. Unfortunately, as of May 20th, AT2023hpb became unobservable under all three filters, rendering the corresponding data set unusable and therefore abandoned.

Table 2: Reference stars data

Reference Stars	RA (J2000)	Dec (J2000)	Mag.	O-C pos	O-C mag	FWHM	Round	S/N	PSNR
1	00:52:51.242	-73:06:53.67	10.916	0.17	0.11	5.44	0.41	856.0	81
2	00:51:30.906	-73:01:23.17	10.534	0.08	0.04	5.36	0.43	978.3	82
3	00:53:09.925	-73:13:24.62	10.866	0.20	0.07	5.52	0.41	791.1	80
4	00:52:27.383	-73:15:06.75	11.747	0.11	0.00	5.54	0.44	485.6	73

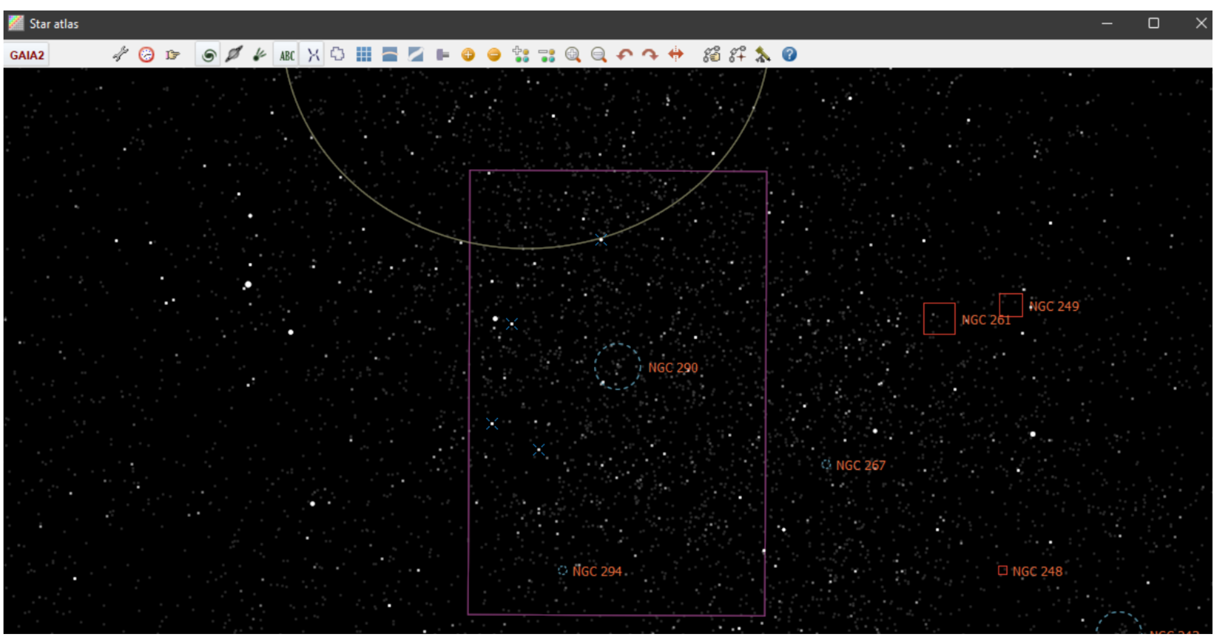

Figure 1: Photometric Data with Uncertainty for filter i

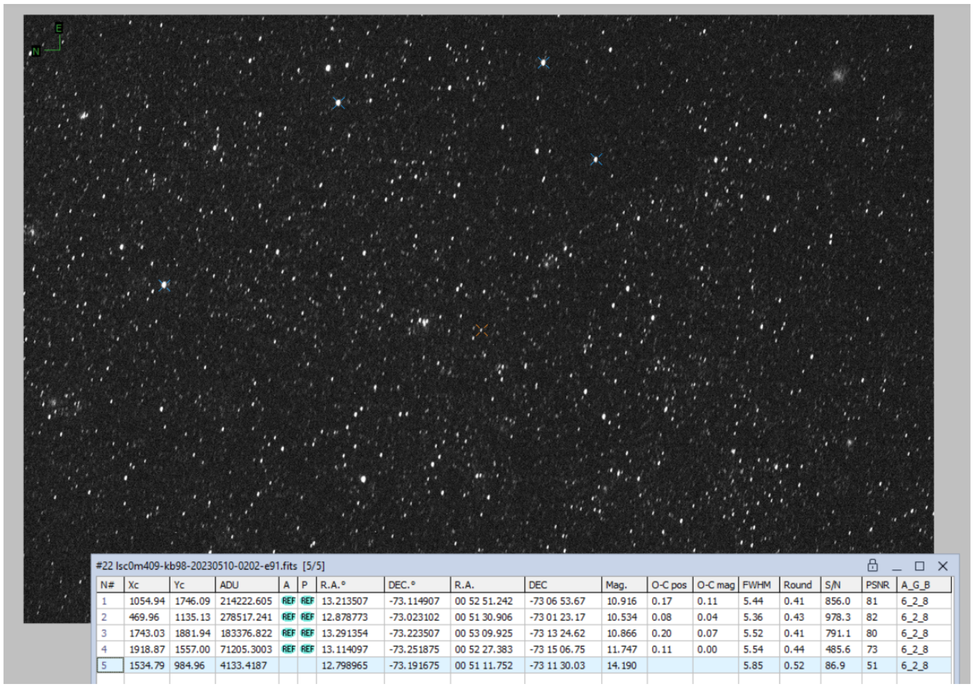

#22 lsc0m409-kb98-20230510-0202-e91.fits [5/5]

N#	Xc	Yc	ADU	A	P	R.A.°	DEC.°	R.A.	DEC	Mag.	O-C pos	O-C mag	FWHM	Round	S/N	PSNR	A_G_B
1	1054.94	1746.09	214222.605	REF	REF	13.213507	-73.114907	00 52 51.242	-73 06 53.67	10.916	0.17	0.11	5.44	0.41	856.0	81	6_2_8
2	469.96	1135.13	278517.241	REF	REF	12.878773	-73.023102	00 51 30.906	-73 01 23.17	10.534	0.08	0.04	5.36	0.43	978.3	82	6_2_8
3	1743.03	1881.94	183376.822	REF	REF	13.291354	-73.223507	00 53 09.925	-73 13 24.62	10.866	0.20	0.07	5.52	0.41	791.1	80	6_2_8
4	1918.87	1557.00	71205.3003	REF	REF	13.114097	-73.251875	00 52 27.383	-73 15 06.75	11.747	0.11	0.00	5.54	0.44	485.6	73	6_2_8
5	1534.79	984.96	4133.4187			12.798965	-73.191675	00 51 11.752	-73 11 30.03	14.190			5.85	0.52	86.9	51	6_2_8

Figure 2: Photometric Data with Uncertainty for filter i

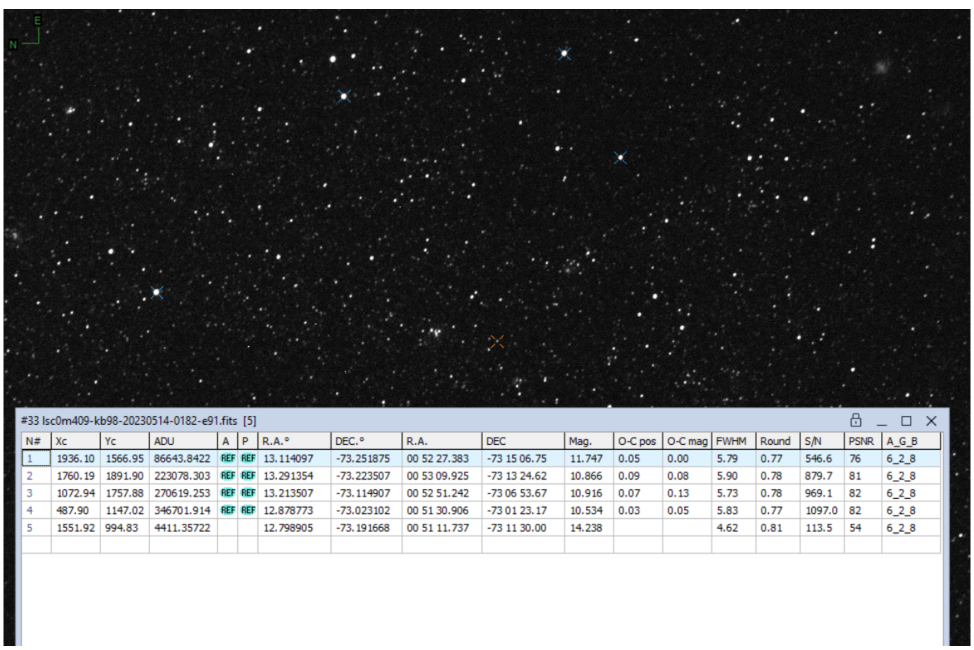

#33 lsc0m409-kb98-20230514-0182-e91.fits [5]

N#	Xc	Yc	ADU	A	P	R.A.°	DEC.°	R.A.	DEC	Mag.	O-C pos	O-C mag	FWHM	Round	S/N	PSNR	A_G_B
1	1936.10	1566.95	86643.8422	REF	REF	13.114097	-73.251875	00 52 27.383	-73 15 06.75	11.747	0.05	0.00	5.79	0.77	546.6	76	6_2_8
2	1760.19	1891.90	223078.303	REF	REF	13.291354	-73.223507	00 53 09.925	-73 13 24.62	10.866	0.09	0.08	5.90	0.78	879.7	81	6_2_8
3	1072.94	1757.88	270619.253	REF	REF	13.213507	-73.114907	00 52 51.242	-73 06 53.67	10.916	0.07	0.13	5.73	0.78	969.1	82	6_2_8
4	487.90	1147.02	346701.914	REF	REF	12.878773	-73.023102	00 51 30.906	-73 01 23.17	10.534	0.03	0.05	5.83	0.77	1097.0	82	6_2_8
5	1551.92	994.83	4411.35722			12.798905	-73.191668	00 51 11.737	-73 11 30.00	14.238			4.62	0.81	113.5	54	6_2_8

Figure 3: Photometric Data with Uncertainty for filter i

3 Data Processing

3.1 Raw Data Processing

Following the aforementioned procedure, we acquired the raw data for all three filters, which is presented in Tables 3.

Table 3: Photometric Data for AT2023hpb

Filter	Date (Observatory)	Magnitude	FWHM	Round	S/N	PNSR	A_G_B
		Filter i					
i	May 10 (LSC)	14.257	3.81	0.89	200.4	67	6_2_8
i	May 11 (LSC)	14.377	3.66	0.91	188.5	65	6_2_8
i	May 13 (LSC)	14.389	4.06	0.99	206.3	67	6_2_8
i	May 14 (LSC)	14.380	4.30	0.81	193.3	64	6_2_8
i	May 15 (LSC)	14.493	4.94	0.9	185.1	65	6_2_8
i	May 16 (LSC)	14.584	4.39	0.93	192.8	66	6_2_8
i	May 17 (COJ)	14.901	3.40	0.94	270.1	71	6_2_8
i	May 18 (LSC)	14.585	4.25	0.91	197	66	6_2_8
i	May 19 (COJ)	14.395	6.12	0.86	170.8	65	6_2_8
i	May 20 (LSC)	N/A					
		Filter g					
g	May 10 (LSC)	14.026	4.77	0.52	99.1	53	6_2_8
g	May 11 (LSC)	14.190	5.85	0.52	86.9	51	6_2_8
g	May 13 (LSC)	14.284	4.90	0.82	113.8	53	6_2_8
g	May 14 (LSC)	14.151	4.23	0.83	134.1	57	6_2_8
g	May 15 (LSC)	14.238	4.62	0.81	113.5	54	6_2_8

Continued on next page

Table 3 – Continued from previous page

Filter	Date (Observatory)	Magnitude	FWHM	Round	S/N	PNSR	A_G_B
g	May 16 (LSC)	14.214	4.31	0.85	141.4	57	6_2_8
g	May 17 (COJ)	14.229	3.55	0.82	201.5	62	6_2_8
g	May 18 (LSC)	14.238	3.90	0.81	146.9	57	6_2_8
g	May 19 (COJ)	13.609	6.79	0.92	139.1	57	6_2_8
g	May 20 (LSC)	N/A					
			Filter r				
r	May 10 (LSC)	14.430	4.07	0.95	242.6	64	6_2_8
r	May 11 (LSC)	14.507	3.61	0.88	223.5	63	6_2_8
r	May 13 (LSC)	14.549	4.26	0.91	246.5	65	6_2_8
r	May 14 (LSC)	14.449	4.38	0.9	249	65	6_2_8
r	May 15 (LSC)	14.547	5.10	0.88	223.2	64	6_2_8
r	May 16 (LSC)	14.666	4.55	0.87	243.7	65	6_2_8
r	May 17 (LSC)	15.083	3.36	0.97	351	71	6_2_8
r	May 18 (COJ)	14.735	4.13	0.84	244.9	65	6_2_8
r	May 19 (COJ)	14.267	5.94	0.71	218.8	63	6_2_8
r	May 20 (LSC)	N/A					

To assess the signal-to-noise ratio (SNR), we utilized Professor Lubin's course notes and applied the corresponding equation. The SNR values provided by Astroart are displayed in the aforementioned tables.

$$\frac{S}{N} = \frac{FA_\varepsilon\sqrt{\tau}}{\left[\frac{N_R^2}{\tau} + FA_\varepsilon + i_{DC} + F_\beta A_\varepsilon \Omega\right]^{1/2}} = \frac{FA_\varepsilon\sqrt{\tau}}{\left[\frac{N_R^2}{\tau} + N_T\right]^{1/2}} = \frac{FA_\varepsilon \tau}{\left[N_R^2 + \tau N_T\right]^{1/2}}.$$

To calculate the photometric uncertainties for each image, Castro's equation was employed. Subsequently, we obtained the photometric data for AT2023hpb, along with their respective uncertainties, as depicted in the subsequent tables.

$$\sigma_{m_{\text{inst}}} = \frac{2.5}{\ln(10)} \frac{\sigma_I}{I} = \frac{2.5}{\ln(10)} \frac{N}{S} \tag{1}$$

Table 4: Photometric Data with Uncertainty for Filters i, g, and r

Filter	Date (Site)	Magnitude	Uncertainty
Filter i			
i	May 10 (LSC)	14.257	0.0054
i	May 11 (LSC)	14.377	0.0058
i	May 13 (LSC)	14.389	0.0053
i	May 14 (LSC)	14.380	0.0056
i	May 15 (LSC)	14.493	0.0059
i	May 16 (LSC)	14.584	0.0056
i	May 17 (COJ)	14.901	0.0040
i	May 18 (LSC)	14.585	0.0055
i	May 19 (COJ)	14.395	0.0064
Filter g			
g	May 10 (LSC)	14.026	0.0110
g	May 11 (LSC)	14.190	0.0125
g	May 13 (LSC)	14.284	0.0095
g	May 14 (LSC)	14.151	0.0081
g	May 15 (LSC)	14.238	0.0096
g	May 16 (LSC)	14.214	0.0077
g	May 17 (COJ)	14.229	0.0054
g	May 18 (LSC)	14.238	0.0074

Continued on next page

Table 4 – Continued from previous page

Filter	Date (Site)	Magnitude	Uncertainty
g	May 19 (COJ)	13.609	0.0078
	Filter r		
r	May 10 (LSC)	14.430	0.0045
r	May 11 (LSC)	14.507	0.0049
r	May 13 (LSC)	14.549	0.0044
r	May 14 (LSC)	14.449	0.0044
r	May 15 (LSC)	14.547	0.0049
r	May 16 (LSC)	14.666	0.0045
r	May 17 (LSC)	15.083	0.0031
r	May 18 (COJ)	14.735	0.0044
r	May 19 (COJ)	14.267	0.0050

3.2 Data Analysis

Based on the aforementioned magnitude data of AT2023hpb under the i, g, and r filters, along with error analysis, we can construct its light curve for the observed period. Notably, to establish a positive correlation between the horizontal axis and the luminosity of AT2023hpb, we reversed the sign of the apparent magnitude.

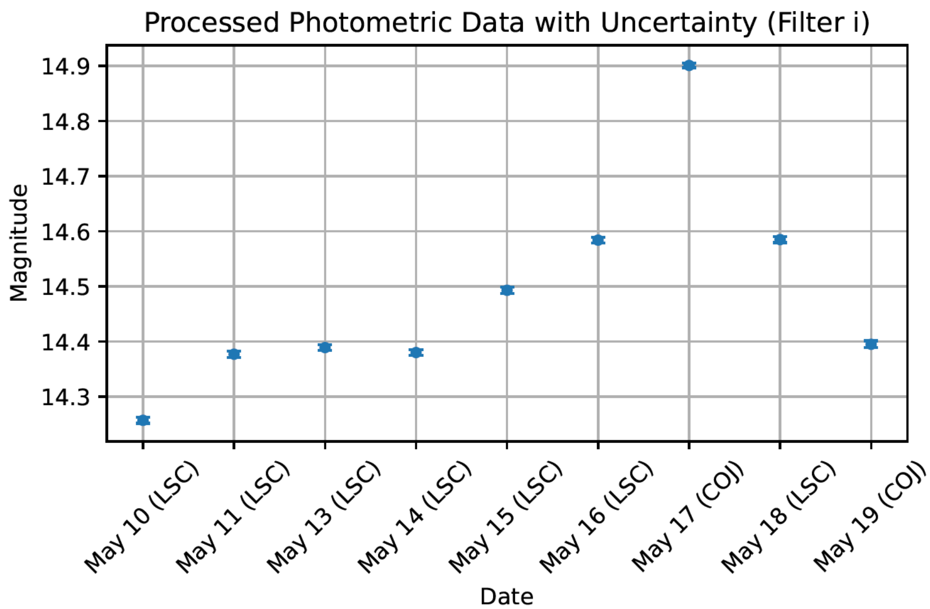

Figure 4: processed Photometric Data with Uncertainty(filter i)

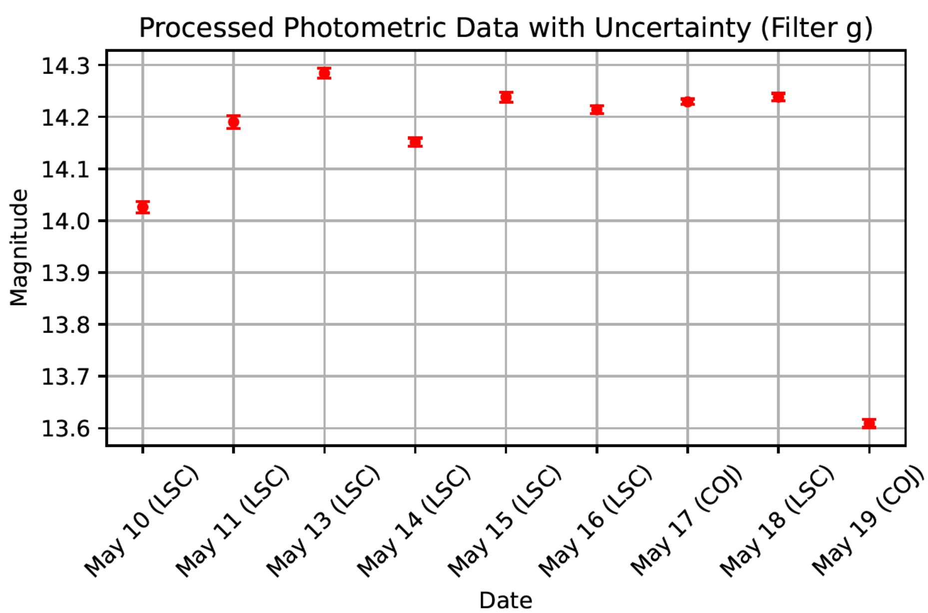

Figure 5: processed Photometric Data with Uncertainty(filter g)

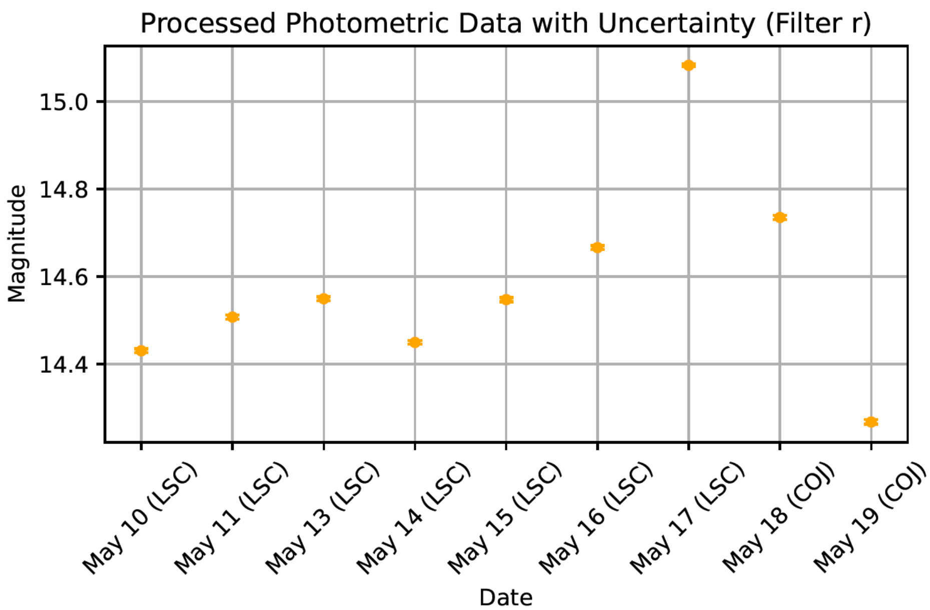

Figure 6: processed Photometric Data with Uncertainty(filter r)

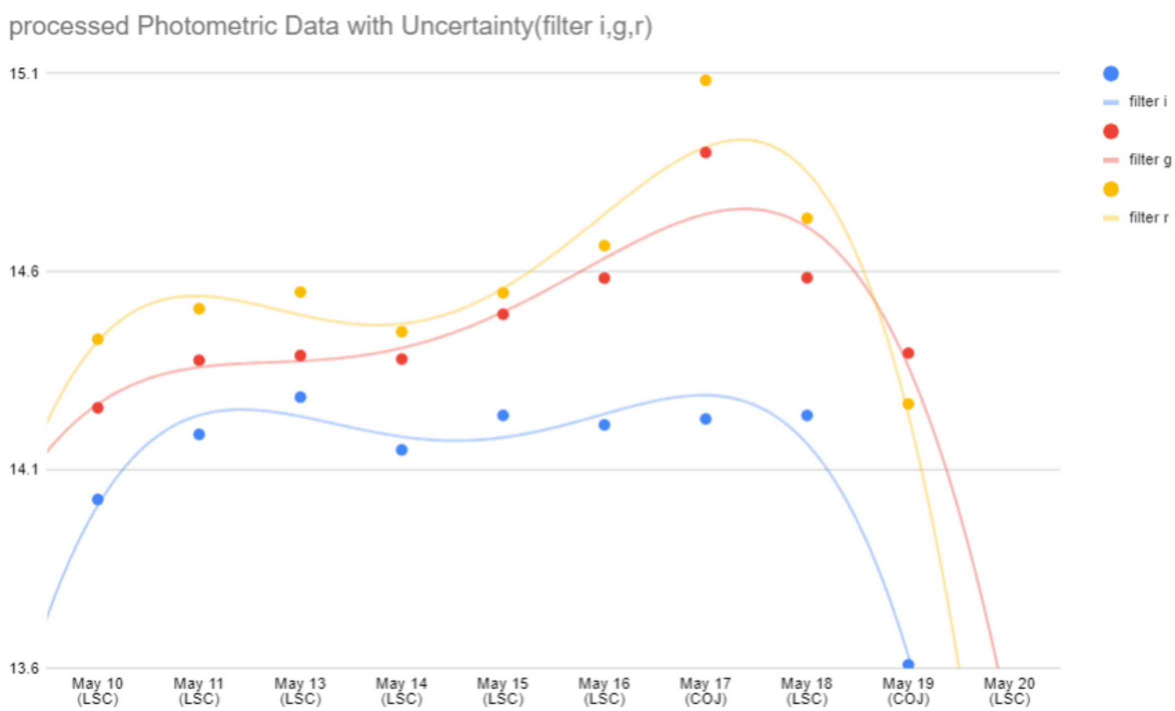

Figure 7: processed Photometric Data with Uncertainty(filter i,g,r)

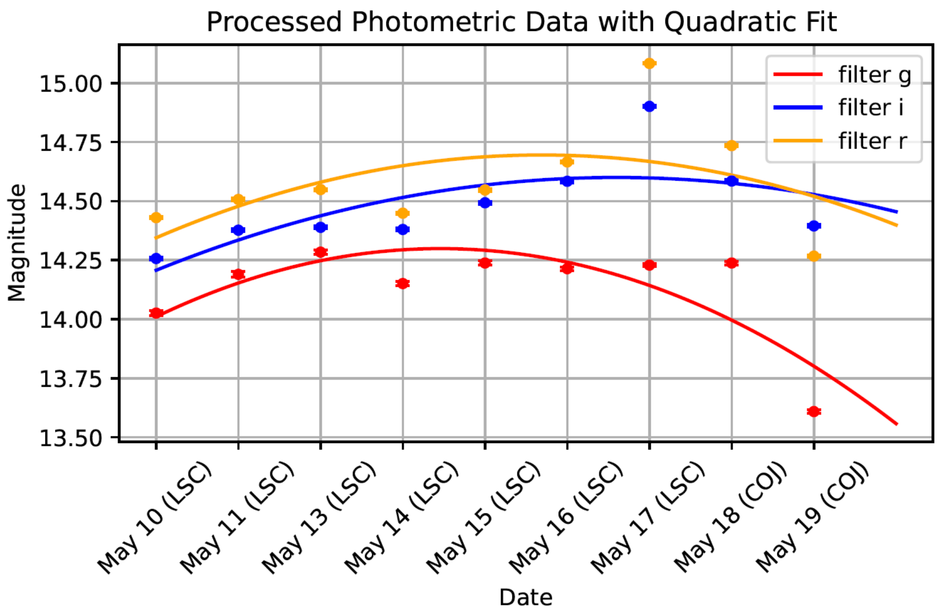

Figure 8: processed Photometric Data with quadratic fit

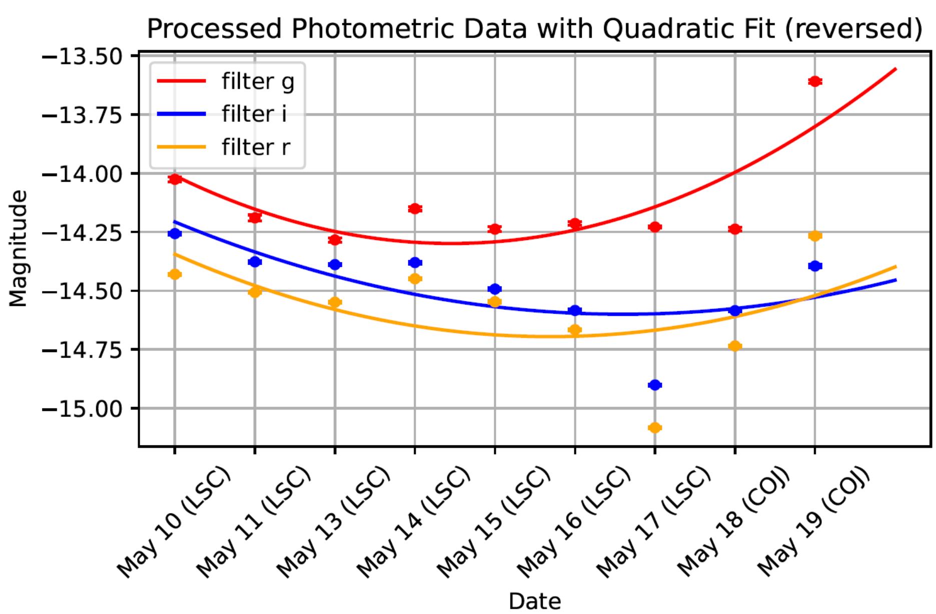

Figure 9: processed Photometric Data with quadratic fit(reversed)

Due to the relatively short observation time, we were unable to capture a complete and clearly regular pattern of the supernova light curve for AT2023hpb. However, it is worth noting that we observed a distinct increase in brightness following a period of decline. Upon revisiting the different types of supernova light curves, we found that this characteristic behavior is predominantly associated with type II supernovae. Therefore, it is reasonable to suggest that AT2023hpb belongs to the type II supernova category based on this observation.

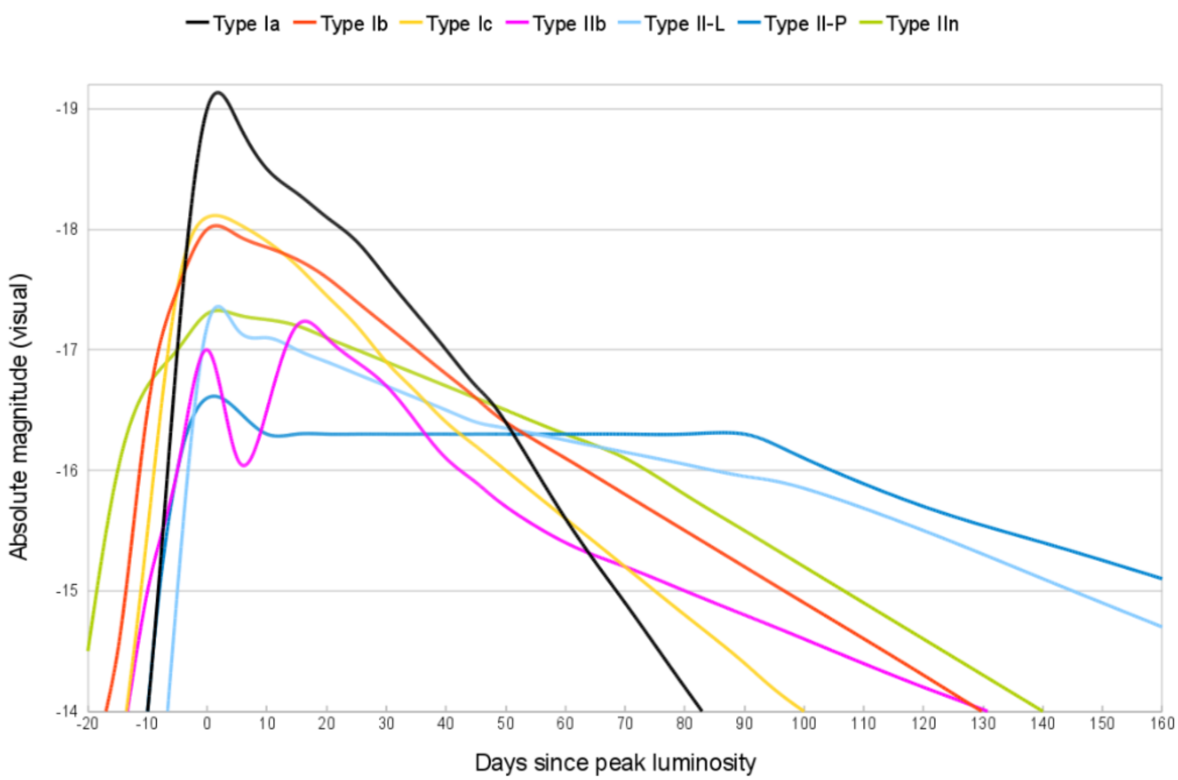

Figure 10: Supernova Light Curve Types

4 Discussion

In this study, we conducted observations of the supernova AT2023hpb and analyzed its light curve over a period of 9 days. The light curve exhibited an initial decline in brightness followed by a subsequent increase. Although our observation period was relatively short, there are several possible explanations for this observed behavior.

One possible explanation is the presence of a secondary peak or bump in the light curve. Supernova light curves can exhibit complex and diverse behaviors, and the presence of secondary peaks or bumps has been observed in some cases. These secondary features can arise from various physical processes, such as interaction with circumstellar material or additional energy input from fallback material . Further analysis and longer observation periods would be necessary to confirm the presence of a secondary peak in the light curve of AT2023hpb.

Another factor that could contribute to the observed behavior is the interaction of the supernova with its surrounding environment. Supernovae occur within a dynamic and evolving medium, and their interaction with the circumstellar material can influence their light curves. In particular, the presence of a dense circumstellar medium can cause the light curve to exhibit irregular or non-monotonic behavior. Our short observation period may have captured only a portion of the interaction phase, leading to the observed fluctuations in brightness. Continued monitoring of the supernova over an extended period would provide valuable insights into the nature of its circumstellar environment and its impact on the light curve .

It is worth noting that our observations were conducted with a specific set of observational parameters, including exposure time and image preprocessing techniques. These parameters can affect the quality and accuracy of the obtained data. To further improve the signal-to-noise ratio and enhance the precision of the light curve analysis, adjustments can be made. Increasing the exposure time would allow for a greater accumulation of photons, leading to improved signal strength and reduced noise. Additionally, implementing advanced image preprocessing techniques, such as image stacking or image registration, can enhance the quality of the obtained images and mitigate systematic errors.

In conclusion, our study provides valuable insights into the light curve behavior of the supernova AT2023hpb during a relatively short observation period. The observed fluctuations in brightness may be attributed to various factors, including the presence of a secondary peak or the interaction of the supernova with its circumstellar environment. Further analysis and longer observation periods are needed to validate these hypotheses. Moreover, optimizing the observational parameters and techniques can lead to improvements in the signal-to-noise ratio and enhance the accuracy of future light curve analyses.

5 Summary

In conclusion, this study focused on the analysis of supernova light curves of AT2023hpb. By examining the changes in magnitude over time, the study provided insights into the behavior and characteristics of supernovae. The observation of an initial decline in brightness followed by a subsequent increase in the light curve of AT2023hpb suggests that it is likely a type 2 supernova. The analysis underscored the importance of light curve analysis in understanding and classifying supernovae. Moreover, it highlighted the need for longer observation periods and advanced observational techniques to further explore the complex nature of supernova behavior. The findings contribute to our knowledge of supernovae and reinforce the significance of light curves in unraveling the mysteries of these celestial events.

References

[1] Filippenko, A. V. (1997). Optical Spectra of Supernovae. Annual Review of Astronomy and Astrophysics, 35, 309-355.

[2] Heger, A., et al. (2003). How Massive Single Stars End Their Life. The Astrophysical Journal, 591(1), 288-300.

[3] Hillebrandt, W., & Niemeyer, J. C. (2000). Type Ia Supernova Explosion Models. Annual Review of Astronomy and Astrophysics, 38, 191-230.

[4] Gal-Yam, A. (2012). Luminous Supernovae. Science, 337(6097), 927-932.

[5] Branch, D., et al. (1995). The Absolute Magnitude of Type Ia Supernovae. The Astrophysical Journal Letters, 441, L33-L36.

[6] Tonry, J. L., et al. (2003). Cosmological Results from High-z Supernovae. The Astrophysical Journal, 594(1), 1-24.

[7] Mazzali, P. A., et al. (2008). A Neutron-star-driven X-ray Flash associated with Supernova SN 2006aj. Science, 321(5886), 1185-1188.

[8] Folatelli, G., et al. (2010). Bolometric Light Curves and Explosion Parameters of 38 Stripped-Envelope Core-Collapse Supernovae. The Astronomical Journal, 139, 120-144.

[9] Riess, A. G., et al. (1998). Observational Evidence from Supernovae for an Accelerating Universe and a Cosmological Constant. The Astronomical Journal, 116, 1009-1038.

[10] Astier, P., et al. (2006). The Supernova Legacy Survey: Measurement of m, and w from the First Year Data Set. Astronomy & Astrophysics, 447, 31-48.

[11] Perlmutter, S., et al. (1999). Measurements of and from 42 High-Redshift Supernovae. The Astrophysical Journal, 517(2), 565-586.

[12] Davis, T. M., et al. (2007). Scrutinizing Exotic Cosmological Models Using ESSENCE Supernova Data Combined with Other Cosmological Probes. The Astrophysical Journal, 666(2), 716-725.

[13] Phillips, M. M. (1993). The Absolute Magnitude of Type Ia Supernovae. The Astrophysical Journal Letters, 413, L105-L108.

[14] Kasen, D., et al. (2009). The Diversity of Type Ia Supernovae from Broken Symmetries. Nature, 460(7259), 869-872.

[15] Purdue University Supernova Database, *http://www.astro.purdue.edu/ salim/astro610/sne.html*

[16] Transient Name Server, AT2023hpb, *https://www.wis-tns.org/object/2023hpb*

[17] Transient Name Server, AT2023hpb Details, *https://www.wis-tns.org/object/2023hpb/details*